Journal of Molecular Liquids 275 (2019) 535–543

Contents lists available at ScienceDirect

Journal of Molecular Liquids

journal homepage: www.elsevier.com/locate/molliq

Physico – chemical properties of $(MgF_2 – CaF_2 – (LiF))_{eut}$ – MgO system as a molten electrolyte for Mg electrowinning

Michal Korenko [a,b,*], Fratišek Šimko [a], Jarmila Mlynáriková [a], Carol Larson [b], Eva Mikšíková [a], Jozef Priščák [a], Marta Ambrová [c], Robert Palumbo [b,d]

[a] Institute of Inorganic Chemistry, Slovak Academy of Sciences, Dúbravská cesta 9, Bratislava 84536, Slovakia
[b] Valparaiso University, 1700 Chapel Dr., Valparaiso, IN 46383, USA
[c] Faculty of Chemical and Food Technology, Slovak University of Technology in Bratislava, Radlinského 9, Bratislava 81237, Slovakia
[d] University of Minnesota Duluth, 1049 1305 Ordean Court, Duluth, MN 55812, USA

ARTICLE INFO

Article history:
Received 24 August 2018
Received in revised form 5 November 2018
Accepted 14 November 2018
Available online 16 November 2018

Keywords:
Solubility of MgO
Electrical conductivity
Density
Viscosity
$MgF_2 – CaF_2 – (LiF))_{eut}$
Molten fluorides

ABSTRACT

Phase diagrams (solubility), density, electrical conductivity and viscosity of molten system $(MgF_2 – CaF_2)_{eut}$ – MgO have been investigated. The phase diagram of $(MgF_2 – CaF_2 – LiF)_{eut}$ – MgO and $(MgF_2 – BaF_2)_{eut}$– MgO and the density of $(MgF_2 – CaF_2 – LiF)_{eut}$ – MgO have been also investigated. The solubility of MgO was measured by means of thermal analysis, the density by means of a computerized Archimedean method, electrical conductivity by means of a tube–cell (pyrolytic boron nitride) with stationary electrodes and the viscosity of the melt by computerized torsion pendulum method. It was found that the all investigated properties varied linearly with temperature in all investigated mixtures. On the basis of density values, the molar volume of the melts and partial molar volume have been calculated. The coordinates of the eutectic systems has been established as follows: $(CaF_2 – MgF_2)_{eut}$ – MgO as 0.30 mol% at 972 °C; $(CaF_2 – MgF_2 – LiF)_{eut}$ – MgO as 0.20 mol% at 941 °C; and $(MgF_2 – BaF_2)_{eut.}$ – MgO as 0.25 mol% at 883 °C. The density of the molten system of $(CaF_2 – MgF_2)_{eut}$ – MgO was found to be at 1000 °C: 2.687 $g \cdot cm^{-3}$ for the system with 0 mol% of MgO; 2.700 $g \cdot cm^{-3}$ for the system with 0.30 mol% of MgO and 2.728 $g \cdot cm^{-3}$ for the system with 0.50 mol% of MgO. The density of the molten system of $(CaF_2 – MgF_2 – LiF)_{eut}$ – MgO was found to be at 1000 °C: 2.875 $g \cdot cm^{-3}$ for the system with 0 mol% of MgO; 2.690 $g \cdot cm^{-3}$ for the system with 0.20 mol% of MgO and 2.650 $g \cdot cm^{-3}$ for the system with 0.30 mol% of MgO. The viscosity of basic eutectic mixture of $(CaF_2 – MgF_2)_{eut}$ at 1000 °C was found to be 7.806 mPa·s.

1. Introduction

Inorganic molten salts are non–aqueous ionic solvents and solutions, which are interesting both from the point of view of fundamental research as well as with regard to their use in industry. One finds them used in the industrial production of aluminum, magnesium, alkali and refractory metals, lanthanides and actinides. They function as solvents in iron and steel metallurgy; specifically, they form slags of the impurities, thereby facilitating their removal in the steel production process. Molten electrolytes are used in galvanic–metal plating as well as in the glass production industry [1–4].

Molten mixtures of alkali metal halides are also planned to be used as solvents for the extraction of nuclear fuel. They are anticipated as being the cooling, as well as a liquid fuel medium for the Molten Salts Rector concept, which is a new type of Generation IV reactor family. In high temperature solar technology, molten salts are also considered as a heat transfer medium, but also as a thermal storage medium for concentrated sunlight. We find molten salts as electrolytes also in fuel cells and batteries, or in high temperature electrolytic reprocessing of spent nuclear fuel [4].

To rank the relevance of a particular system for an industrial application, an in–depth knowledge and analysis of a molten salt's physio–chemical behavior is indispensable. It is imperative that the option of a proper melt for a specific application, which is often a multi–component mixture, is set by the requisite optimum of the physio–chemical performance (at a given temperature) in relation to the given economical context of the process.

In this study, we bring forth our physico–chemical findings for molten salts consisting of mixtures of MgF_2, CaF_2, BaF_2, LiF, for the dissolution of MgO at temperatures ranging from circa 940–1100 °C. Although the work has broad relevance to the vast number of current and developing industrial processes that use or may use molten halide systems, our motivation for doing this work was narrow: the development of a new process for producing Mg from MgO. We think it is instructive for the reader to appreciate our motivational context.

* Corresponding author at: Institute of Inorganic Chemistry, Slovak Academy of Sciences, Dúbravská cesta 9, Bratislava 84536, Slovakia.
E-mail address: michal.korenko@savba.sk (M. Korenko).

https://doi.org/10.1016/j.molliq.2018.11.066
0167-7322/

Palumbo et al. [5], Leonard et al. [6] and Korenko et al. [7] have recently developed a new, eco–economic, electrochemical–thermal process for the effective production of magnesium (Mg) from magnesium oxide (MgO) that works between 975 and 1025 °C. Magnesium is produced in the process by the following electrochemical reaction:

$$2\,MgO(diss) + C(s) \rightarrow 2\,mg(l) + CO_2(g) \quad (1)$$

The electrochemical reagent MgO, dissolved in a molten eutectic mixture of MgF_2 – CaF_2, is electrolyzed to liquid Mg and gaseous CO_2. The Mg(l) forms at a cathode and the CO_2(g) forms at a consumable solid carbon anode C(s). This concept may reduce capital and operating costs and reduce the environmental impact of primary Mg production compared to the conventional $MgCl_2$ electrolysis process and thermal Pidgeon processes, the latter process being responsible for *ca* 90% of the world market.

The Pidgeon processes requires at least 133 MJ/kg–Mg of energy and releases of 26 kg CO_2/kg–Mg [8]. In comparison, the production of steel needs less than 36 MJ/kg and results in the release of less than 3 kg CO_2/kg–steel [9]. A more environmentally friendly and energy efficient process to produce magnesium is thus highly desirable.

In the work Palumbo et al. [5] and Leonard et al. [6], basic features of the proposed technology are summarized. Leonard et al. [6] presents the requisite fundamental kinetic and mass transport parameters. The reactions kinetics (exchange current densities, transfer coefficients) for the anode and cathode and the diffusion coefficients for the electroactive species were established.

In the work Korenko et al. [7], a technical and economic evaluation of a solar thermal Mg production is presented. The authors evaluate from techno–economic view a 17,000–18,000 metric ton per year electrolytic process with and without concentrated solar thermal input. In this analysis, the molten fluoride high temperature electrolysis is combined with a solar thermal input to reduce environmental and operating costs. Energy requirements as well as resulting CO_2 production per kg of Mg for that process were based on the extrapolation of the thermodynamic, kinetic and transport parameters established in Leonard et al. [6].

The goal of this work is to offer a set of physico–chemical data of the electrolyte's system mentioned in the title of this work, so that the data can be used to further advance physical, chemical and economical assessments of this new industrial magnesium electrowinning process. The primary electrolyte system for this technology (eutectic mixture of MgF_2 – CaF_2 with MgO as electroactive species) has been identified based on the current efficiency analysis of magnesium produced by electrolysis [5]. The current efficiency based on magnesium has been identified as high enough (80–95%) and is considered as industrially viable [5].

Using a molten fluoride electrolyte system in this particular technology has some advantages (over e.g. traditionally used molten chlorides in current magnesium electrolysis). The molten fluorides have relatively low partial pressure, they are less hygroscopic than molten chlorides and they tend to be good solvents of oxides. Another advantage of molten fluorides, particularly important for high temperature solar applications, is their wide range of thermal stability.

Despite the wide use of molten fluorides in aluminum industry, there is, however, relatively limited information about the physico–chemical behavior of MgF_2 – CaF_2 – MgO system in the open literature. There are some papers dealing with the phase diagram of the eutectic system of MgF_2 – CaF_2 (Rolin and Clausier [10], Berezhnaya and Bukharova [11] and Barton et al. [12]). Only Martin and West [13] reported a visual observation study of MgO solubility in some molten salts, but not in our system. Some works related to the high temperature (1250–1600 °C) measurement of electrical conductivity of the eutectic system MgF_2 – CaF_2 can be found in Voronin et al. [14], Kim and Sadoway [15] and Goncharov et al. [16]. The temperature range of these measurements is however substantially higher than the temperature of our process.

In this light, this paper focuses on the need for thorough analysis to understand, predict and optimize the physical properties of the molten fluoride systems that could be applied to new Mg production electrolytic technology and obtain the data necessary to support industrial reactor design/development. We will present in this work the physico–chemical data of the primary electrolyte system (eutectic mixture of MgF_2 – CaF_2 with MgO), including solubility of MgO in the electrolyte, density, electrical conductivity and viscosity. Besides the primary electrolyte we will also present the data of the electrolyte modified by some additives (LiF and BaF_2).

All the data presented in this paper are original data with one exception. The data of the electrical conductivity has been already published in the work Leonard et al. [6]. We include these data in to this work for a practical reason to have in one place all related data of physico–chemical analysis of the molten fluoride electrolyte for magnesium electrowinning.

2. Experimental

The following chemicals have been used in the experiments: MgF_2 (99.9%, Chempur), CaF_2 (Merck 99.8%), MgO (Aldrich, 99.8%), LiF (99.9%, Sigma–Aldrich) and BaF_2 (Merck 99.8%). CaF_2, MgF_2 and MgO were dried at 500 °C for 4 h. All chemicals were handled inside a high purity argon atmosphere (99.9990%, Messer Tatragas) in a glove box (water content\10 ppm).

2.1. Solubility measurements

The minimal solubility of MgO in molten fluoride electrolyte systems was determined by means of thermal analysis. 10 g of a very well homogenized mixture of oxide and solvent was put into a platinum crucible and the crucible was placed in an electrical resistance furnace. The furnace atmosphere was Ar. A Pt — Pt10Rh thermocouple was embedded into the mixture for establishing the temperature vs. time trace. The accuracy of the thermocouple was established by comparing the measured melting temperatures of pure salts (NaCl, KCl) to the thermocouple output. With this calibration the uncertainty of the temperature measurement was determined to be ±2 °C with a confidence level of 95%.

The thermal analysis was conducted with a heating rate of 5 °C·min^{-1} and cooling rate of 1.5 °C·min^{-1}. Fig. 1 is an example of a typical cooling curve. The cooling curves were used for the determination of the temperature of primary crystallizations and the eutectic temperatures in all systems, except for the system modified by BaF_2, where the

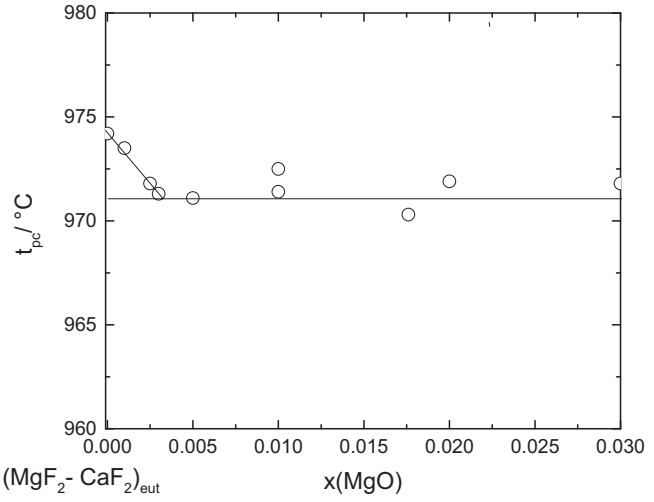

Fig. 1. Cross–section of the ternary phase diagram of the system $(CaF_2 – MgF_2)_{eut}$ – MgO. Y– axis represents the eutectic mixture of $(CaF_2 – MgF_2)_{eut}$.

heating curves were used due to the super—cooling effect detected in this mixture. Further information about the procedure can be found elsewhere [17–18].

2.2. Electrical conductivity

The electrical conductivity was measured with the well—established electrochemical impedance spectroscopy method, using a cell made of a pyrolytic boron nitride (pBN, Boralloy, Momentive™) capillary and platinum—rhodium electrodes. The diameter of the pBN capillary was 4 mm, the length was 100 mm and the thickness of the wall of the capillary was 0.5 mm. The pBN capillary works here as a sheath for one of the electrodes made of Pt10Rh alloy. A crucible, made of the same alloy, was used as a counter electrode and as a container for the measured salt mixture. The BN tube with the Pt10Rh electrode was immersed into the measured salt mixture in such a way that the distance between the end of the electrode inside the BN tube and the bottom of the crucible, which works as second electrode, was always the same.

35 g of the investigated salts mixture was usually used for the measurement. The uncertainty of the Pt — Pt10Rh thermocouple was found to be ±2 °C. An impedance/gain phase analyzer (National Instruments™), controlled by Labview software, was used to measure the cell impedance. NaCl and KCl were used for the determination of the cell constant. The uncertainty of the conductivity measurement was found to be ±3% of the reading with a confidence level of 95%. Further details of the method and the uncertainty analysis can be found elsewhere [18–19].

2.3. Density

The Archimedean method was used for the determination of the density of the molten systems. A platinum pendulum, suspended on a platinum wire, attached to an electronic balance, was used as the measuring body. The technique is based on the measured weight of the pendulum immersed in the molten samples compared to the weight of the pendulum not immersed. The measurement was calibrated using a NaCl and KF mixture of known density. The temperature was measured using a Pt — Pt10Rh thermocouple. The LabView software environment was used for controlling the measurements and data collecting. The uncertainty of the measurement was found to be ±0.5% of the reading with a confidence level of 95%. More details about the technique can be found in the following works [18,20–24].

2.4. Viscosity

The computerized torsion pendulum method with logarithmic decrement attenuation due to the friction in the melt was used for the viscosity measurement. A platinum cylinder (outer diameter 15 mm and the height of 20 mm) was used as the measuring body. Oscillations of the pendulum driven by a servomotor were registered by two phototransistors, placed in the path of a light beam reflected from a mirror connected to the pendulum. The oscillations of the pendulum in a liquid with a certain viscosity represent dumping harmonic oscillations. So the dumping of the oscillations will be more pronounced in a more viscous melt. The pendulum is always immersed at the same depth. LabView software controlled the servomotor and gathered the oscillation data. The most important variables are the logarithmic decrement of dumping and the period of oscillations. The uncertainty in the viscosity measurement was established by comparing our system output for the molten NaCl and KF system to that published in the literature for this salt mixture. The uncertainty in the viscosity data was found to be ±2.5% of the reading. The technique is described in more detail in Daněk's monography [18].

3. Results

3.1. Solubility measurements

The solubility of metal oxides as a source of electro–active species in electrolyte is of primary importance, since the low solubility of the source of the metal could be a killing point for any electrolytic industrial technology. We have already proven in our previous work [5–7], without having more information about the different aspects of the chemistry of electrolyte, that the technology, which is based on MgO dissolved in molten fluoride electrolyte, has industrial potential. This study represents an attempt to know more about the physical chemistry of electrolyte.

The phase diagrams are the manifestation of the thermodynamics of the systems. The points in phase diagrams represent stops (changes in the cooling rate) on the experimental cooling curves of the thermal analysis. Figs. 1–3 show the cross–sections of the phase diagrams of the systems under the investigation. The phase diagrams contain in all cases three planes. In general, the plane above the horizontal line is a region where all the components are in melted state. The plane bellow the horizontal line represents the region where all the components are in solid phase. A "triangular" plane, at the horizontal line, represents the region of coexistence of the crystals of the solid mixture of MgF_2 – CaF_2 (Fig. 1), CaF – MgF_2 – LiF (Fig. 2), and MgF_2 – BaF_2 (Fig. 3) and the melt of these solvents with the MgO.

The horizontal line in the phase diagrams is related with the ternary eutectic systems (e.g. $(CaF_2 – MgF_2) – MgO)_{eut}$ and $(MgF_2 – BaF_2)_{eut}$ – MgO), or quaternary eutectic system in the case of $(CaF_2 – MgF_2 – LiF)_{eut}$ – MgO. The point, where all regions in a phase diagram meet, represents the solubility of MgO in the respective binary/ternary eutectic solvent at the indicated temperature. This point is a point in the phase diagram when the primary crystallization line meets the horizontal line (line of the points where the change of the composition had no effect on the temperature of phase transition detected in the experiment).

The horizontal line in our phase diagrams is not identical with a "truly" ternary eutectic temperature (quaternary in the case of CaF_2 – MgF_2 – LiF – MgO). The "truly" ternary/quaternary eutectic temperature in this case means the eutectic of entire ternary/quaternary system (e.g. $(CaF_2 – MgF_2 – LiF)_{eut}$ – MgO is just sub–system the entire quaternary CaF_2 – MgF_2 – LiF – MgO).

As it can be seen, the solubility of MgO in all investigated systems is very low. The eutectic points in all investigated systems, represent the solubility of MgO at related temperature.

Based on the measured data, we predict the coordinates of the ternary/quaternary eutectic of the measured systems i) $(CaF_2 – MgF_2)_{eut}$ – MgO as 0.3 mol% at 972 °C, ii) $(CaF_2 – MgF_2 – LiF)_{eut}$ – MgO as

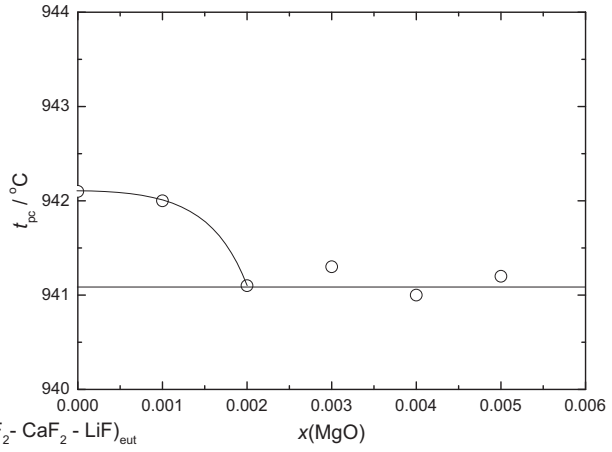

Fig. 2. Cross–section of the quaternary phase diagram of the system $(CaF_2 – MgF_2 – LiF)_{eut}$ – MgO. Y– axis represents the eutectic mixture of $(CaF_2 – MgF_2 – LiF)_{eut}$.

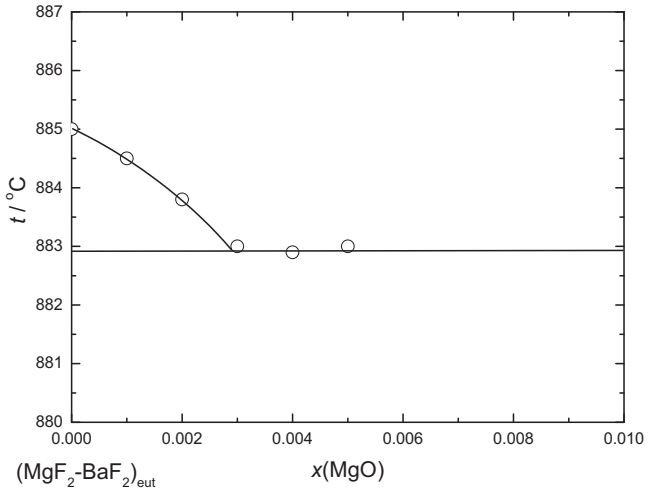

Fig. 3. Cross–section of the ternary phase diagram of the system $(MgF_2 – BaF_2)_{eut}$ – MgO. Y– axis represents the eutectic mixture of $(MgF_2 – BaF_2)$.

0.2 mol% at 941 °C and iii) $(MgF_2 – BaF_2)_{eut}$ – MgO as 0.25 mol% at 883 °C. Further addition of MgO beyond the mentioned concentration has no influence on the temperature of the primary crystallization of the investigated eutectic mixtures. Thus, the aforementioned coordinates of these eutectics represent the maximum concentration of MgO at this temperature in these molten systems.

These findings are in agreement with the work Martin and West [13] where the solubility of magnesium oxide in a variety of molten salts was determined by a visual method. Only mixtures containing cryolite or sodium metaphosphate were found to dissolve more than 0.2% of magnesium oxide.

The low solubility of MgO in a fluoride melt is of concern if the goal is to produce Mg by electrolysis: The anode could be starved of MgO and cell voltages could rise to levels that break down the fluoride melt as the cell tries to maintain a given desired current level. In our previous works [6–7], we, however, found that MgO has a high enough dissolution rate in the $MgF_2 – CaF_2$ electrolyte system, so we were able to maintain anode current densities of circa 0.5 $A \cdot cm^{-2}$ (a temperature range of the electrolysis was 980–1025 °C).

In terms of modifying of our electrolyte by some additives, it is quite clear, from our findings, that neither addition of LiF, nor substitution of BaF_2 will have significant positive effect on the solubility of MgO in molten electrolyte.

3.2. Density

In the electrolytic production of metals, especially when two or more liquids are involved, the density of molten electrolyte influences the design of the cells. Specifically how a liquid product is separated from the electrolyte depends on whether the product rises or sinks. The density is also important for fundamental reasons. The experimentally determined density data serve as a basis in the study of volume properties of molten electrolytes. Simultaneously, the density measurement is also one of the indirect methods used in the study of the structure of molten salts.

The temperature dependence of the density for all our investigated systems was expressed in the form of the linear equation:

$$\rho = a + bt \tag{2}$$

where ρ/g·cm^{-3} is density, t/°C is temperature and coefficients a/g·cm^{-3} and b/g·cm^{-3} °C^{-1} are constants along with the standard deviations of approximations, obtained by the linear regression analysis of experimentally obtained data.

Some information about the chemistry and the structure of the mixture can be gained from volume properties. The volume of two–component systems can be written as follows. For simplicity we consider our systems as two component, where one component is the basic eutectic mixture $(MgF_2 – CaF_2)_{eut}$ (solvent) and the another is MgO (solute).

$$dV = \left(\frac{\partial V}{\partial T}\right)_{P,n_1,n_2} dT + \left(\frac{\partial V}{\partial P}\right)_{T,n_1,n_2} dP + \left(\frac{\partial V}{\partial n_1}\right)_{T,P,n_2} dn_1 + \left(\frac{\partial V}{\partial n_2}\right)_{T,P,n_1} dn_2 \tag{3}$$

T is the thermodynamic temperature, P is the pressure and n_i is the amount of component in the mixture. Partial derivations by amount of each components (from Eq. (3)) are partial molar volumes and are marked as $\overline{V_1}$ and $\overline{V_2}$

$$\overline{V_2} = \left(\frac{\partial V}{\partial n_2}\right)_{T,P,n_1} \tag{4}$$

The partial molar volume physically is the volume expansion/contraction due to the addition of 1 mol of component in to the infinite amount of the solution. A partial molar volume can thus be a positive or a negative value.

At constant temperature and pressure, and in a one mole mixture ($dx_1 = -dx_2$), the partial molar volume is given by

$$\overline{V_2} = V_m + x_1\left(\frac{\partial V_m}{\partial x_2}\right) \tag{5}$$

where V_m is the molar volume of the mixture. The molar volume of a two–component system can be obtained from the experimentally measured density (ρ_{exp}) and molar weights of each component (M_i) with Eq. (6).

$$V_m = \frac{x_1 M_1 + x_2 M_2}{\rho_{exp}} \tag{6}$$

The concentration dependence of molar volume was fitted to a multicomponent polynomial using a regression analysis. The details of this approach are given in detail in references [21–23].

3.2.1. Density of molten $CaF_2 – MgF_2 – MgO$

In this section we will present the results related to the density of molten system $CaF_2 – MgF_2 – MgO$. The density of the molten electrolyte with addition of LiF will be present in the next section.

The experimental data of the density as a function of temperature is shown in Fig. 4. Each compositions on the figure (0, 0.03, 0.05 mol% of MgO) represents two or three independent runs. The density linearly decreases with the temperature. The slope of the decrease is slightly steeper for the system with the highest composition of MgO.

Table 1 summarizes the regression coefficients a/g·cm^{-3} and b/g·cm^{-3} °C^{-1} for calculation of the density of $(MgF_2 – CaF_2)_{eut}$ – MgO system (according Eq. (2)) and the standard deviation of the regression coefficients. The table also contains the calculated density at 1000 °C and its standard deviation.

The molar volume of the mixture, partial molar volume of the MgO and the partial molar volume of MgO in infinite diluted mixture calculated from the experimental data are listed in the Table 2. The composition dependence of molar volume of the system of $MgF_2 – CaF_2)_{eut}$ – MgO is shown in the Fig. 5.

As it can be seen, the molar volume of the mixture decreases with the increased concentration of MgO in the eutectic mixture of $MgF_2 – CaF_2$.

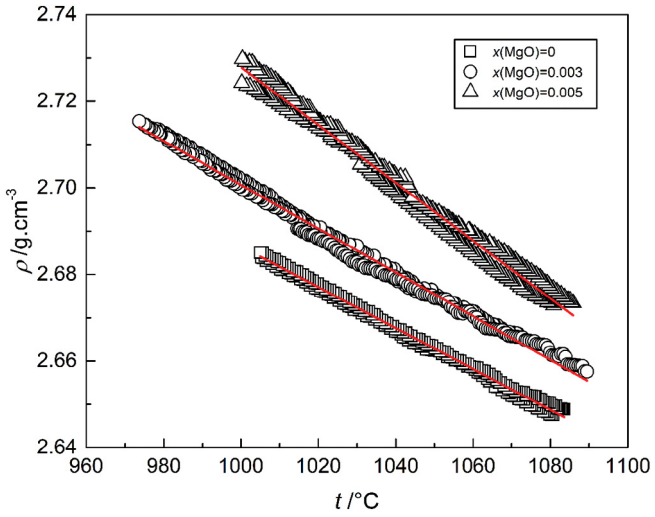

Fig. 4. Results of the density measurements of the molten system $(MgF_2 - CaF_2)_{eut}$ – MgO. Each composition represents two independent runs. Line: average calculated based on Eq. (2).

3.2.2. Density of molten $CaF_2 - MgF_2 - LiF - MgO$

The experimental data of the density as a function of temperature is shown in Fig. 6. The density in all cases decreases with increasing temperature.

Table 3 summarizes the regression coefficients for $a/g\cdot cm^{-3}$ and $b/g\cdot cm^{-3}\,°C^{-1}$ for calculation of density of the $(MgF_2 - CaF_2 - LiF)_{eut}$ – MgO system (Eq. (2)) and the standard deviation of the regression coefficients.

The molar volume of the mixture, partial molar volume of the MgO and the partial molar volume of MgO in infinite diluted mixture calculated from the experimental data are listed in the Table 4. The composition dependence of molar volume of the system of $(MgF_2 - CaF_2 - LiF)_{eut}$ – MgO is shown in the Fig. 7. The molar volume linearly increase with the MgO concentration in the melt.

As one can see from Figs. 4 and 6 (and also from Figs. 5 and 7), the influence of the addition of MgO on the density of both systems is different. Whereas in the system $(MgF_2 - CaF_2)_{eut}$, the addition of MgO to this eutectic system has a small positive influence on the density (*ca* up to 1%), in the system with LiF ($(MgF_2 - CaF_2 - LiF)_{eut}$) has addition of MgO a negative influence (*ca* by 7–9%). It means that the composition dependence of molar volume in these systems is different. While in the system without LiF, molar volume decreases with the concentration of MgO in the melt, this is opposite in the system with LiF.

The explanation for the different behaviour of MgO in these systems, probably lies within the different nature of the internal structure of both melts. Whereas in the system without LiF, MgO creates complex species approximately of the same size as other constituents of the melt, in the

Table 2
Molar volume ($V_m/cm^3\cdot mol^{-1}$) and partial molar volume of MgO ($\overline{V}_{m,MgO}/cm^3\cdot mol^{-1}$) and partial molar volumes of MgO at infinite dilution ($\overline{V}^{,T}_{m,MgO}/cm^3\cdot mol^{-1}$) for the system $(MgF_2 - CaF_2)_{eut}$ – MgO at temperatures 1000 °C; x_1 is $(MgF_2 - CaF_2)_{eut.}$; x_2 is MgO.

$V^t_m/cm^3\cdot mol^{-1}$	$\overline{V}^t_{m,MgO}/cm^3\cdot mol^{-1}$	$\overline{V}^{,t}_{m,MgO}/cm^3\cdot mol^{-1}$
$V_m^{1000\,°C} = 26.10x_1 + 54.74x_2 - 18606.26x_1^3x_2^2$	$\overline{V}_{m,MgO}^{1000\,°C} = 54.74 + 37212.52x_1^3 - 111637.56x_1^4 + 74425.04x_1^5$	$\overline{V}_{m,MgO}^{1000\,°C} = 54.74$

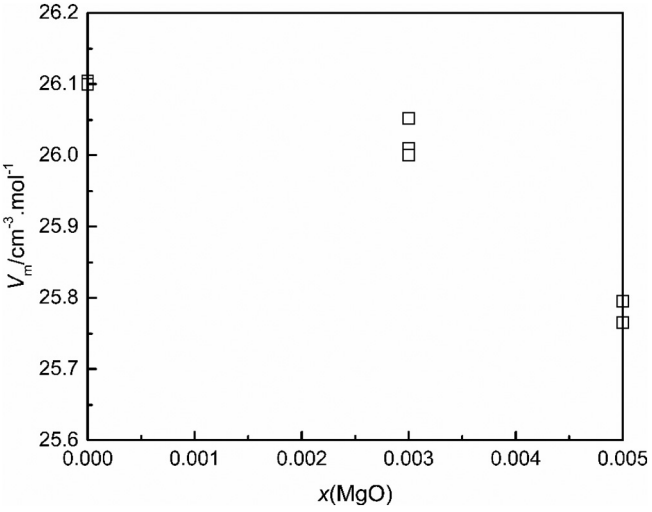

Fig. 5. Molar volume $V_m/cm^3\cdot mol^{-1}$ of the molten systems $(MgF_2 - CaF_2)_{eut}$ – MgO, 1000 °C.

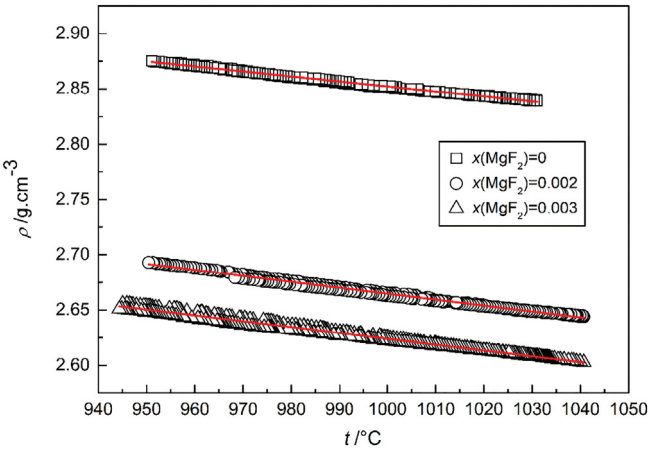

Fig. 6. Results of the density measurements of the molten system $(MgF_2 - CaF_2 - LiF)_{eut}$ – MgO. Each composition represents two independent runs. Line: average calculated based on Eq. (2).

Table 1
Results of the density measurement of molten system $(MgF_2 - CaF_2)_{eut}$ – MgO in the form of Eq. (1).

x(MgO)	$\frac{t}{°C}$	$\frac{a}{g\cdot cm^{-3}}$	$\frac{\sigma a}{g\cdot cm^{-3}}$	$\frac{b\times10^{-4}}{g\cdot cm^{-3}\cdot °C^{-1}}$	$\frac{\sigma b\times10^{-6}}{g\cdot cm^{-3}\cdot °C^{-1}}$	$\frac{\rho^{1000\,°C}}{g\cdot cm^{-3}}$	$\frac{\sigma\rho^{1000\,°C}}{g\cdot cm^{-3}}$
0	1000–1080	3.168	0.002	−4.820	1.5	2.686	0.002
0	1000–1080	3.154	0.002	−4.676	1.7	2.687	0.002
average	1000–1080	3.161	0.002	−4.748	1.6	2.687	0.002
0.03	978–1045	3.204	0.002	−5.028	1.8	2.701	0.003
0.03	973–1070	3.128	0.002	−4.314	2.3	2.696	0.003
0.03	1010–090	3.265	0.001	−5.637	1.4	2.702	0.002
average	973–1090	3.199	0.002	−4.993	1.8	2.700	0.003
0.05	1000–1080	3.403	0.003	−6.771	3.2	2.726	0.005
0.05	1000–1080	3.391	0.003	−6.619	3.0	2.730	0.004
average	1000–1085	3.397	0.003	−6.695	3.1	2.728	0.004

Table 3
Results of the density measurement (based on the Eq. (2)) of molten system $(MgF_2–CaF_2 – LiF)_{eut}$ – MgO.

x(MgO)	$\frac{t}{°C}$	$\frac{a}{g·cm^{-3}}$	$\frac{\sigma a}{g·cm^{-3}}$	$\frac{b\times10^{-4}}{g·cm^{-3}·°C^{-1}}$	$\frac{\sigma b\times10^{-6}}{g·cm^{-3}·°C^{-1}}$	$\frac{\rho^{1000\,°C}}{g·cm^{-3}}$	$\frac{\sigma\rho^{1000\,°C}}{g·cm^{-3}}$
0	960–1020	3.302	0.004	−4.498	3.8	2.875	0.005
0	950–1020	3.306	0.001	−4.534	1.5	2.875	0.002
average	950–1020	3.304	0.003	−4.516	2.7	2.875	0.004
0.02	950–1040	3.222	0.002	−5.564	1.8	2.693	0.002
0.02	970–1040	3.143	0.002	−4.795	1.7	2.687	0.002
average	950–1040	3.183	0.002	−5.180	1.8	2.690	0.002
0.03	950–1030	3.191	0.001	−5.659	1.2	2.653	0.002
0.03	940–1000	3.111	0.002	−4.883	1.9	2.647	0.003
average	940–1030	3.151	0.002	−5.271	1.6	2.650	0.003

Table 4
Molar volume (V_m/cm^3 · mol^{-1}) and partial molar volume of MgO ($\overline{V}_{m,MgO}$/cm^3 · mol^{-1}) and partial molar volumes of MgO at infinite dilution ($\overline{V}^{,t}_{m,MgO}$/cm^3 · mol^{-1}) for the system $(MgF_2–CaF_2 – LiF)_{eut}$ – MgO at temperatures 1000 °C; x_1 is $(MgF_2 – CaF_2 – LiF)_{eut}$; x_2 is MgO.

V^t_m/cm^3 · mol^{-1}	$\overline{V}^t_{m,MgO}$/cm^3 · mol^{-1}	$\overline{V}^{,t}_{m,MgO}$/cm^3 · mol^{-1}
$V_m^{1000\,°C} = 23.04x_1 + 1090.58x_1x_2 - 139621.80x_1^2x_2^2$	$\overline{V}_{m,MgO}^{1000\,°C} = 140712.38x_1^2 - 558487.20x_1^3 + 418865.40x_1^4$	$\overline{V}_{m,MgO}^{1000\,°C} = 1090.58$

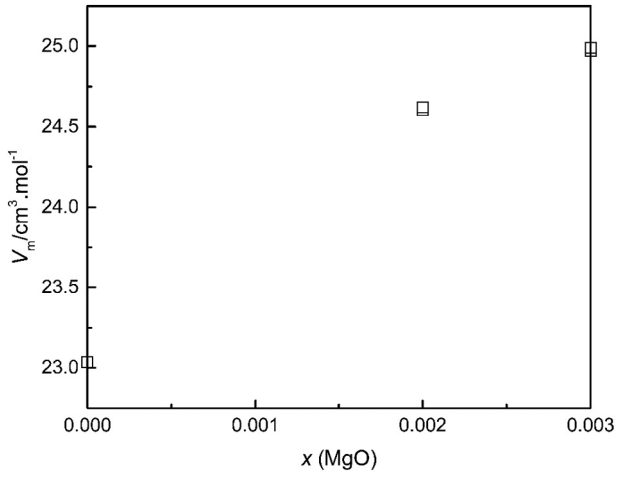

Fig. 7. Molar volume V_m/cm^3 · mol^{-1} of the molten systems $(MgF_2 – CaF_2 – LiF)_{eut}$ – MgO, 1000 °C.

system with LiF, MgO creates the complex species of different size and that fact is probably responsible, in this case, for more visible change of density. We hypothesize, based on the analogy with the cryolite chemistry in aluminum industry, that the electroactive species in both system are complex anions of the same nature (oxofluoro complexes). This is due to the solvation of the metal oxide in the molten fluoride electrolyte [1]. In fact, we have found in our previous work [6] an electrochemical correlation (cyclic voltammetry on anode graphite electrode) between our technology and the cryolite electrolysis used in aluminum industry. There are many similarities between both technologies: the reactant for both systems is a metal oxide; the electrolyte of both systems is a fluoride salt, both systems operate near 1000 °C, and the anode is graphite.

3.3. Electrical conductivity

The experimental data of the electrical conductivity of the molten system $CaF_2 – MgF_2 – MgO$ are presented as a function of temperature and composition of the electrolyte (Fig. 9). The values have been formally fit by a least squares second order polynomial regression analysis.

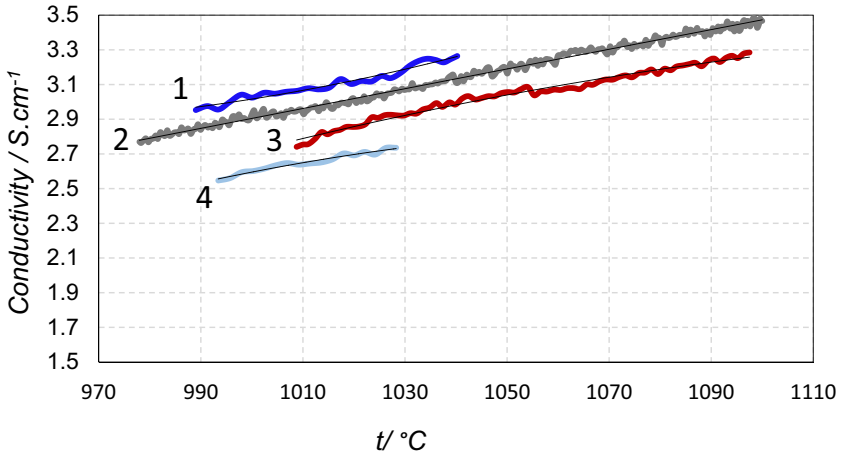

Fig. 8. Conductivity of the molten system $MgF_2 – CaF_2 – MgO$ as a function of temperature. (1) – $(MgF_2 – CaF_2)_{eut}$ + 0.3 mol% MgO; (2) – $(MgF_2 – CaF_2)_{eut}$ (3) – $(MgF_2 – CaF_2)$ with higher concentration of MgF_2, $x(MgF_2) = 55$ mol%; (4) – $(MgF_2 – CaF_2)_{eut}$ + 1 mol% MgO. The data have been formally fit by a least squared second order polynomial regression.

Table 5
Regression coefficients *a* and *b* and standard deviations of the viscosity Eq. (7) of the molten system $(MgF_2 - CaF_2)_{eut}$.

No.	$x(MgF_2)$	$x(CaF_2)$	$\frac{t}{°C}$	$\frac{a}{mPa·s}$	$\frac{\sigma a}{mPa·s}$	$\frac{b}{mPa·s·°C}$	$\frac{\sigma b}{mPa·s·°C}$
1	0.504	0.496	1000–1080	−2.587	0.230	4709	250
2	0.504	0.496	1001–1080	−1.986	0.221	4034	231
3	0.504	0.496	1002–1080	−1.863	0.168	3863	177
average	0.504	0.496	1000–1080	−2.145	0.207	4202	220

The conductivity of all the measured systems increase with the temperature. The conductivity of the blank electrolyte (without MgO) is 2.9 $S·cm^{-1}$ at 1000 °C, which is *ca* 5% higher than the conductivity of pure molten cryolite (2.8 $S·cm^{-1}$) – the major component of the electrolyte in aluminum industry.

The curve 3 in the Fig. 8 shows the values of the conductivity in the molten system $MgF_2 - CaF_2$ ($x(MgF_2) = 55$ mol%) where the ratio of the MgF_2/CaF_2 was slightly shifted from the eutectic mixture toward a higher concentration of MgF_2. The reason was to see the influence of the change of the ratio on the conductivity.

As can be seen, an increase of the concentration ratio of MgF_2/CaF_2 has a negative influence on the conductivity of the molten electrolyte. An increase of the concentration of MgF_2 in the mixture will probably have positive influence on conductivity. We have to however take in to account that the change of the composition will also increase the temperature of primary crystallization of the electrolyte.

The system $(MgF_2 - CaF_2)_{eut}$ with an addition of 0.3 mol% of MgO (which is about the solubility of MgO in this system) has increased the conductivity to 3 $S·cm^{-1}$. However, a further increase of MgO has a negative influence on the conductivity (2.6 $S·cm^{-1}$) of the molten fluoride electrolyte. Addition of MgO beyond the saturation limit likely reduces the conductivity forming a suspension of MgO solid particles which impede the current convection paths in the molten electrolyte.

Our results extend the work of others. There are only a few papers with the electrical conductivity of the binary alkaline–earth fluoride molten melts. Voronin et al. [14] and Kim and Sadoway [15] studied electrical conductivity of SrF_2 –MgF_2, $BaF_2 - MgF_2$, $CaF_2 - MgF_2$ systems, Ogino et al. [25] studied $CaF_2 - MgF_2$ and $CaF_2 - BaF_2$, Izmolin et al. [26] studied systems of $CaF_2 - MgF_2$, CaF_2 – LiF and CaF_2 – LiF – NaF and Goncharov et al. [16] $CaF_2 - MgF_2$. In this work, there is also the data of the system $CaF_2 - MgF_2$ – MgO. However, the MgF_2/CaF_2 ratio reported, circa 25/75 by weight, is far away from the eutectic composition. Furthermore all of the reported works were performed at higher temperatures (1250–1600 °C). Nonetheless the electrical conductivity from our work extrapolates well to the results reported by Sadoway and Kim [15]. The difference between the conductivity of the eutectic mixture is 0.29 $S·cm^{-1}$ at 1473 °C.

3.4. Viscosity

The viscosity of the electrolyte in any electrolytic process may influence several of the hydrodynamic parameters of the cell, like convection in the electrolyte and liquid metal, the sedimentation of undissolved oxide particles, the rate of mixing and solution of oxide in the electrolyte and release of gas bubbles from anode working surface.

The viscosity, like electrical conductivity, is one of the transport properties. Since the molten salt are composed of two kinds of particles that have a different radius, we may expect that the viscosity will be given by motion of the bigger and more slow ions. This effect may have been seen in particular in melts containing complex ions, which are much bigger than the present cations. Due to this fact the viscosity and electrical conductivity of this melts cannot be correlated. Similarly, the activation energy of viscous flow are often higher than those of electrical conductivity.

The viscosity of water at 20 °C is 1.009 mPa·s. The viscosity of molten cryolite electrolyte used industrially for aluminum production at 1000 °C is 2.3 mPa·s [1]. The viscosity of liquids depends significantly on temperature, it can change even by some orders of magnitude. The temperature dependence of viscosity is thus most often expressed in the form of exponential equation

$$\ln\{\eta\}/\mathrm{mPas} = a + b/t \tag{7}$$

where $\ln\{\eta\}$ is a logarithm of dynamic viscosity and *a* and *b* the coefficients. The Eq. (7) is just one of the forms of the well–known Arrhenius equation

$$\eta = \eta_0 \ \exp\left(\frac{E}{RT}\right) \tag{8}$$

where *R* is universal gas constant ($J·mol^{-1}·K^{-1}$), *T* is thermodynamic temperature (K), *E* is activation energy ($J·mol^{-1}$) and η_0 is a constant (Pa·s).

Table 5 presents the experimental results of the viscosity of the basic eutectic system $MgF_2 - CaF_2$ in the form of Eq. (7). We have measured this systems three times. The experimental data of viscosity as a function of temperature are depicted in Fig. 9. The viscosity at 1000 °C is calculated from Eq. (7) and the data from all three runs listed in Table 6. The activation energy of the viscous flow was for this system calculated as 35 ± 3 $kJ·mol^{-1}$. It can also be seen that the viscosity of this system is relatively high. Our electrolyte is almost four times more viscous (7.8 mPa·s at 1000 °C), when compare to the viscosity of the electrolyte used in aluminum industry (2.3 mPa·s at 1000 °C [1]).

In some molten fluoride systems reported in the works [27–28], more dramatic changes of the viscosity with temperature has been reported. The temperature relationship of the viscosity could show a local maximum(s) or minimum(s) attributed to the internal structural changes of the melt structure. Bulavin [27] reported a formation of some clusters with covalent bonds in the system NaF–LiF–NdF_3. Our

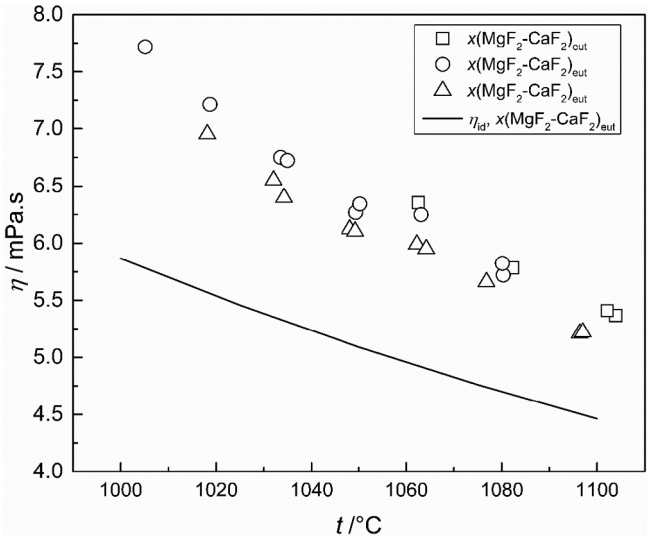

Fig. 9. Temperature dependence of viscosity of the system $(MgF_2 - CaF_2)_{eut}$, three different runs. The full line: additive model.

Table 6
Results of the viscosity measurement of molten system $(MgF_2 – CaF_2)_{eut}$ in the form of Eq. (6), 1000 °C.

No.	$x(MgF_2)$	$w(MgF_2)$	$x(CaF_2)$	$w(CaF_2)$	$\frac{\ln \eta^{1000\ °C}}{mPa \cdot s}$	$\frac{\eta^{1000\ °C}}{mPa \cdot s}$
1	0.504	0.448	0.496	0.552	2.122	8.345
2	0.504	0.448	0.496	0.552	2.049	7.759
3	0.504	0.448	0.496	0.552	2.000	7.386
average	0.504	0.448	0.496	0.552	2.057	7.830

results, in fact, oppose any such behavior in our investigated temperature range. The reason is probably complete ionic character of our melt.

The ideal viscosity of the studied system has also been calculated based on the additive model (line in Fig. 9). The additive model is based on the molar fractions of the viscosities of the pure components of the melt. When the experimental data is compared with the additive model (Fig. 9) the experimental data show a positive deviation from the additive model, which are likely caused by interactions between the components of the melt. The additive model, from principle, are not able to cover the interactions of the components of the melt and their influence on the physico–chemical properties.

A more careful study of the electrolyte's viscosity is likely imperative if one needs to learn how best decrease it (e.g. by some additives or by changing the MgF_2/CaF_2 ratio). We surmise the lowering the viscosity could be important for the operation of the future industrial process. For example our MgO process may require a cell with convective flow, a situation where low viscosity will be critical.

We are currently not able to carry out a more extensive study with better repeatability since our experimental device was not designed for the measurement of such viscous liquids. Our device is limited to fluids with a viscosity near 8 mPa·s. We attribute the limitations of our instrumentation to the high scattering of the experimental data.

Even though we did not measure the viscosity of the electrolyte with electroactive species, we can also reasonable expect that the addition of MgO will further increase the viscosity of our electrolyte. Evidence for such a claim is that adding MgO to levels 10 times above saturation leads to sludge formation. There is great importance to have the complete viscosity data of the electrolyte if the process is to someday be optimized. We are thus planning to upgrade our device for the measurement of more viscous liquids for future work.

4. Conclusions

The solubility of the MgO in $(MgF_2 – CaF_2)_{eut}$, $(MgF_2 – CaF_2 – LiF)_{eut}$, and $(MgF_2 – BaF_2)_{eut}$ has been analyzed by thermal analysis. It can be concluded that the solubility of MgO in these systems is very low compared to the solubility of alumina in cryolite electrolyte, which can be considered as a bench mark for any other possible high temperature industrial electrowinning process of a metal from molten salts. The low solubility in our system however is balanced by rapid dissolution rates of MgO, as shown in our previous works [6–7].

The analysis of volume properties of the systems $(MgF_2 – CaF_2)_{eut}$ – MgO and $(MgF_2 – CaF_2 – LiF)_{eut}$ – MgO revealed a different influence of addition of MgO on the density of these melts. While in the system without LiF, the molar volume decreases with the concentration of MgO in the melt. The opposite effect occurs in the system with LiF. We have hypothesized that the explanation for different behaviour resides with the different nature of the internal structure between melts. Whereas in the system without LiF, MgO creates complex species approximately of the same size as other constituents of the melt, in the system with LiF, MgO creates the complex species of a different size.

In terms of the measurement of electrical conductivity of the CaF_2 – MgF_2 – MgO, we have the following findings. The conductivity of the blank electrolyte ($(MgF_2 – CaF_2)_{eut}$ without MgO) is by *ca* 5% higher than the conductivity of pure molten cryolite (2.8 $S \cdot cm^{-1}$) – the major component of the electrolyte in aluminum industry. A small increase of the concentration of MgO in the melt (0.3 mol%) has positive influence on the conductivity, but the presence of MgO at higher concentration (1 mol%) has had a negative impact on the conductivity. We have also found that the deviation of the ratio of MgF_2/CaF_2 from the eutectic composition toward a higher concentration has a negative effect on the conductivity of the melt.

The viscosity of the eutectic system of MgF_2 – CaF_2 was found to be very close to the detection limit of our measuring device (7.8 mPa·s at 1000 °C). One can see a very large difference between this number and the viscosity of the electrolyte used in aluminum industry (2.3 mPa·s at 1000 °C [1]).

Finally it is important to reflect back on a motivation for doing this study: to obtain the requisite physico – chemical data to optimize our electrochemical process for producing Mg from MgO. To date our process has been shown to plausibly be industrially viable. At the writing of this article, the electrolytic cell described in the introduction is being scaled to operate at hundreds of amperes rather than the 20–30 A described in the literature we sited for this work [5–7]. If we demonstrate that our understanding of cell performance does hold at a large scale, much more in depth modeling – models that account for dissolution rate and the possibility of adding forced convective flow to the cell become important for ensuring the design of an economic process: the physico – chemical data in this article will be essential input into these more sophisticated models.

Acknowledgement

We are grateful to the US Department of Energy ARPA–E program (cooperative agreement DE–AR0000421). This work was also supported by the Slovak Research and Development Agency under the contracts No. APVV–15–0738 and APVV–15–0479, and by the Slovak Grant Agency (VEGA 2/0060/18).

References

[1] J. Thonstad, P. Fellner, G.M. Haarberg, J. Híveš, H. Kvande, Å. Sterten, Aluminium Electrolysis, 3rd. ed. Aluminium – Verlag, Duesseldorf, 2001.
[2] K. Grjotheim, B. Welsh, Aluminium Smelter Technology: A Pure and Applied Approach, Aluminium - Verlag, Duesseldorf, 1988.
[3] K. Grjotheim, H. Kvande, L. Qingfeng, Q. Zhuxian, Metal Production by Molten Salt Electrolysis: Especially Aluminium and Magnesium, China University of Mining and Technology Press, Xuzhou, 1998.
[4] G.D. Lovering (Ed.), Molten Salt Technology, Plenum Press, New York, 1982.
[5] R. Palumbo, M. Korenko, C. Larson, L.J. Venstrom, S. Duncan, S. Nudehi, J. Schoer, J. Toberman, W. Prusinski, D. Johnson, B. Robinson, S. Barkely, K. Waren, R. Diver, F. Simko, M. Boca, Thermal electrolytic production of Mg from MgO: reflections on commercial viability, in: M.V. Manuel, A. Singh, N. Alderman, N.R. Neelameggham (Eds.), Magnesium Technology, John Wiley and Sons, New York, 2015.
[6] N. Leonard, M. Korenko, C. Larson, K. Blood, L.J. Venstrom, S. Nudehi, S. Duncan, R. Diver, F. Simko, J. Priscak, J. Schoer, P.T. Kissinger, R. Palumbo, The thermal electrolytic production of mg from MgO: a discussion of the electrochemical reaction kinetics and requisite mass transport processes, Chem. Eng. Sci. 148 (2016) 155–169.
[7] M. Korenko, C. Larson, K. Blood, R. Palumbo, S. Nudehi, R. Diver, D. Blood, F. Šimko, L.J. Venstrom, Technical and economic evaluation of a solar thermal MgO electrolysis process for magnesium production, Energy 135 (2017) 182–194.
[8] S. Ehrenberger, Life Cycle Assessment of Magnesium Components in Vehicle Construction, DLR Report, German Aerospace Centre, Stuttgart, 2013.
[9] E. Worrell, L. Price, N. Martin, Energy efficiency and carbon dioxide emissions reduction opportunities in the US iron and steel sector, Energy 26 (5) (2001) 513–536.
[10] M. Rolin, M. Le Clausier, Système Fluorure de Calcium Fluorure de Baryum-Fluorure de Magnésium, Rev. Int. Hautes Temp. Refract. 4 (1) (1967) 42–47.

[11] V.T. Berezhnaya, G.A. Bukhanova, The ternary system of Mg, Ca, and Ba fluorides, Zhurnal Neorganicheskoi Khimii, J. Inorg. Chem. (6) (1961) 2136–2138 (Russ).
[12] C.J. Barton, L.M. Bratcher, J.P. Blakely, W.R. Grimes, Unpublished work performed at the Oak Ridge National Lab, Cited according Thoma, R.E. (Ed.) Phase Diagram of Nuclear Reactor Materials; ORNL-2548, Oak Ridge National Laboratory, Oak Ridge, TN 1959, p. 30.
[13] R.L. Martin, J.B. West, Solubility of magnesium oxide in molten salts, J. Inorg. Nucl. Chem. 24 (1) (1962) 105–111.
[14] B.M. Voronin, V.D. Prisyazhnyi, K.K. Khizhnyak, Equivalent electric coductivity of melts of alkaline earth metal and magnesium fluoride, Ukr. Khim. Zh. 584–587 (Russ) (1980) 46.
[15] K.B. Kim, D.R. Sadoway, Electrical conductivity measurements of molten alkaline −earth fluorides, J. Electrochem. Soc. 139 (1992) 1027–1033.
[16] A.E. Goncharov, L.I. Manakov, P.K. Kovalev, Trudy Instituta Matallurgii, Akad. Nauk SSSR 27−32 (1972) 159 (Russ).
[17] F. Simko, V. Danek, Cryoscopy in the system Na_3AlF_6-Fe_2O_3, Chem. Pap. - Chem. Zvesti 55 (2001) 269–272.
[18] V. Daněk, Physicochemical Analysis of Molten Electrolytes, Elsevier, Amsterdam, 2006.
[19] M. Korenko, J. Priscak, F. Simko, Electrical conductivity of systems based on Na_3AlF_6 −SiO_2 melt, Chem. Pap. 67 (2013) 1350–1354.
[20] F. Simko, I. Mackova, Z. Netriova, Density of the systems (NaF/AlF3)-AlPO4 and (NaF/AlF_3)−$NaVO_3$, Chem. Pap. 65 (2011) 85–89.
[21] J. Cibulkova, M. Chrenkova, R. Vasiljev, V. Kremenetsky, M. Boca, Density and viscosity of the $(LiF + NaF + KF)_{(eut)}(1) + K_2TaF_7(2) + Ta_2O_5(3)$ melts, J. Chem. Eng. Data 51 (3) (2006) 984–987.
[22] J. Mlynáriková, M. Boca, V. Gurišová, I. Macková, I. Netriová, Thermal analysis and volume properties of the systems $(LiF–CaF_2)_{eut.}$ –LnF_3 (Ln=Sm, Gd, and Nd) up to 1273 K, J. Therm. Anal. Calorim. 124 (2016) 973–987.
[23] J. Mlynáriková, M. Boca, E. Mikšíková, I. Netriová, Volume properties of the molten systems MF-K_2TaF_7 (MF=LiF, NaF and KF), J. Therm. Anal. Calorim. 129 (2017) 475–486.
[24] Sh. Hara, H. Shibaike, K. Ogino, The molar volume and surface tension of melts in the system CaF_2–*M*F (*M*: Li, Na) and CaF_2–MF_2 (*M*: Mg, Sr, Ba), ISIJ Int. 30 (40) (1990) 298–304.
[25] K. Ogino, H. Hashimoto, H. Hara, Tetsu To Hagane, 64, 1978 225–231 (Jap).
[26] S.A. Izmolin, V.P. Istomin, E.A. Pastukhov, V.V. Ryabov, Razplavy, 6, 2007 10–14 (Russ).
[27] L. Bulavin, Yu. Plevachuk, V. Sklyarchuk, L. Shtablavy, N. Faidiuk, R. Savchuk, J. Nucl. Mater. 433 (2013) 329–333.
[28] L. Bulavin, Yu. Plevachuk, V. Sklyarchuk, A. Omelchuk, N. Faidiuk, R. Savchuk, L. Shtablavy, V. Vus, A. Yakymovych, Nucl. Eng. Des. 270 (2014) 60–64.